

# Evaluation of safety and dosimetry of $^{177}\text{Lu}$ -DOTA-ZOL for therapy of bone metastases

*René Fernández<sup>1</sup>, Elisabeth Eppard<sup>2</sup>, Wencke Lehnert<sup>3,4</sup>, Luis David Jiménez-Franco<sup>3</sup>, Cristian Soza-Ried<sup>1</sup>, Matías Ceballos<sup>1</sup>, Jessica Ribbeck<sup>2</sup>, Andreas Kluge<sup>3</sup>, Frank Rösch<sup>5</sup>, Marian Meckel<sup>6</sup>, Konstantin Zhernosekov<sup>6</sup>, Vasko Kramer<sup>1,2</sup> and Horacio Amaral<sup>1,2</sup>*

<sup>1</sup>Center for Nuclear Medicine & PET/CT Positronmed, Santiago, Chile

<sup>2</sup>Positronpharma SA, Santiago, Chile

<sup>3</sup>ABX-CRO, Dresden, Germany

<sup>4</sup>Department of Nuclear Medicine, University Medical Center Hamburg, Germany

<sup>5</sup>Institute of Nuclear Chemistry, Johannes Gutenberg-University, Mainz, Germany

<sup>6</sup>Isotope Technologies Garching GmbH, Munich, Germany

**KEYWORDS:** Bone metastasis; Bisphosphonate,  $^{177}\text{Lu}$ -DOTA-ZOL, Radionuclide therapy; Dosimetry

**RUNNING TITLE:** Safety and dosimetry of  $^{177}\text{Lu}$ -DOTA-ZOL

Immediate Open Access: Creative Commons Attribution 4.0 International License (CC BY) allows users to share and adapt with attribution, excluding materials credited to previous publications.  
License: <https://creativecommons.org/licenses/by/4.0/>.  
Details: <https://jnm.snmjournals.org/page/permissions>.



## ABSTRACT

Palliative treatment of bone metastasis using radiolabelled bisphosphonates is a well-known concept proven to be safe and effective. A new therapeutic radiopharmaceutical for bone metastasis is  $^{177}\text{Lu}$ -DOTA-Zoledronic acid ( $^{177}\text{Lu}$ -DOTA-ZOL). In this study, safety and dosimetry of a single therapeutic dose of  $^{177}\text{Lu}$ -DOTA-ZOL were evaluated based on a series of SPECT/CT images and blood samples. **Methods:** Nine patients with exclusive bone metastases from metastatic castration-resistant prostate cancer (mCRPC) ( $70.8 \pm 8.4$  y) and progression under conventional therapies participated in this prospective study. After receiving  $5780 \pm 329$  MBq  $^{177}\text{Lu}$ -DOTA-ZOL, patients underwent 3D whole-body SPECT/CT imaging and venous blood sampling over seven days. Dosimetric evaluation was performed for main organs and tumor lesions. Safety was assessed by blood biomarkers. **Results:**  $^{177}\text{Lu}$ -DOTA-ZOL showed fast uptake and high retention in bone lesions and fast clearance from the blood stream in all patients. The average retention in tumor lesions was 0.02 %IA/g at 6 h post-injection (p.i.) and approximately 0.01 %IA/g at 170 h p.i. In this cohort, the average absorbed doses in bone tumor lesions, kidneys, red bone marrow, and bone surfaces were 4.21, 0.17, 0.36, and 1.19 Gy/GBq, respectively. The red marrow was found to be the dose-limiting organ for all patients. A median maximum tolerated injected activity of 6.0 GBq may exceed the defined threshold of 2 Gy for the red bone marrow in individual patients (4/8). **Conclusion:** In conclusion,  $^{177}\text{Lu}$ -DOTA-ZOL is safe and has a favorable therapeutic index compared to other radiopharmaceuticals used in the treatment of osteoblastic bone metastases. Personalized dosimetry, however, should be considered to avoid severe hematotoxicity for individual patients.

## INTRODUCTION

The development of bone metastasis is a well-known complication of prostate cancer in advanced stages. The skeletal metastasis often cause severe symptoms reducing the quality of life of the patients significantly (1). Currently incurable, skeletal metastases considerably contribute to an increased morbidity and mortality (2). Nuclear medicine techniques play a key role in the diagnosis, staging and treatment of the skeletal metastatic disease.

Compared to most other therapeutic beta emitters, lutetium-177 has favorable physical properties ( $T_{1/2}$  6.7 d;  $E_{\beta\max}$  497 keV;  $E_{\gamma}$  113 keV (6.4%), 208 keV (11%)) and proven clinical therapeutic utility (3,4). Moreover, lutetium-177 is commercially available in high specific activities and radionuclide purities. All in all, lutetium-177 is suitable for the treatment of small and medium-sized tumors and allows for dosimetry and individual treatment planning using scintigraphic and single photon emission computed tomography (SPECT) imaging.

Bisphosphonates are a well-known group of drugs used for treatment of bone disease. Several studies investigated  $^{177}\text{Lu}$ -labelled bisphosphonates e.g.  $^{177}\text{Lu}$ -EDTMP (5) or  $^{177}\text{Lu}$ -BPAMD (6). Although  $^{177}\text{Lu}$ -EDTMP proved to have high potential for pain palliation (7–9) as well as favorable radiation dose characteristics compared to other bone targeting drugs (10), its  $^{68}\text{Ga}$ -analogue, with lower accumulation in bone, is not suitable as a diagnostic pair (11). In contrast, the DOTA-conjugate BPAMD showed favorable results when labelled with lutetium-177 and gallium-68, enabling individualized patient treatment (12).

Zoledronic acid, a last-generation bisphosphonate, has shown very high hydroxyapatite affinity and inhibition of the farnesyl diphosphate synthase (13). These properties render it as an ideal candidate for theranostics, leading to the development of DOTA-Zoledronic acid (DOTA-ZOL). Preclinical and first clinical evaluations revealed its high potential (6,10,14,15). Biodistribution and skeletal uptake were found to be comparable for the  $^{68}\text{Ga}$ - or  $^{177}\text{Lu}$ -labelled compounds (10,16,17). Thus,  $^{68}\text{Ga}$ -/ $^{177}\text{Lu}$ -DOTA-ZOL (or even  $^{225}\text{Ac}$ -DOTA-ZOL) provide a set of potential theranostic radiopharmaceuticals, enabling patient-individual dosimetry and pre- and post-therapeutic evaluation.

In this prospective study, dosimetry and safety of a single therapeutic dose of  $^{177}\text{Lu}$ -DOTA-ZOL was evaluated in patients with metastatic castration-resistant prostate cancer (mCRPC) based on a series of SPECT/CT images and blood samples.

## **MATERIALS AND METHODS**

### **Study Design and Patients**

Study approval was obtained from the regional ethics committee board (CEC-SSM-Oriente, permit 20170829). All patients gave written informed consent and all reported investigations were conducted in accordance with the Helsinki Declaration and with local regulations.

Nine male patients ( $70.8 \pm 8.4$  years; range: 57-82 years) were enrolled for  $^{177}\text{Lu}$ -DOTA-ZOL therapy. Patients had received surgery, radiotherapy, first and/or second line androgen deprivation therapy and/or chemotherapy as previous treatments and were on palliative treatment with no other treatment options available at the time of inclusion. The presence of bone metastasis and absence of visceral metastasis was verified by  $^{68}\text{Ga}$ -PSMA-11 ( $n=2$ ) or  $^{18}\text{F}$ -PSMA-1007 ( $n=7$ ) PET/CT scans within one week prior to therapy. Blood biomarkers (Supplemental Tab. 1) were evaluated at the day of treatment (baseline), week 4, and week 10 post-injection (p.i.) (follow-up).  $^{177}\text{Lu}$ -DOTA-ZOL was prepared as previously described (15).  $5780 \pm 329$  MBq (range: 5215-6380 MBq) of  $^{177}\text{Lu}$ -DOTA-ZOL were administered as an intravenous bolus over 6-10 seconds followed by saline flush. One out of nine patients (subject 5) needed to be retrospectively excluded from the dosimetric evaluation due to corruption of the SPECT data. A detailed description of radiosynthesis and patient data is given in the Supplemental Tab. 1.

### **SPECT/CT Imaging and Blood Sampling**

A series of 3D SPECT/CT imaging was performed to evaluate organ and tumor dosimetry. For each patient, whole-body SPECT/CT scans were acquired (three bed positions from the top of the head to the upper thighs; 90 projections and 25 s per projection) on a Symbia T2 scanner (Siemens Healthineers, Germany) at  $1.5 \pm 0.5$ ,  $6 \pm 1$ ,  $24 \pm 3$ ,  $48 \pm 3$  h and at  $7 \pm 1$  d p.i. The scanner was equipped with a medium energy low penetration collimator. Three energy windows were acquired and used for further processing: a peak window of 20% width centered around the 208 keV energy peak and two adjacent corresponding lower and upper scatter energy windows of 10% width each. Quantitative reconstruction of the stitched SPECT images was performed using a 3D ordered subset expectation maximization algorithm with 8 iterations and 9 subsets applying uniformity correction, CT-based attenuation correction, energy-based scatter correction and collimator-detector response modeling.

To yield quantitative images (Bq/mL) a calibration factor was determined from a phantom experiment using an IEC NEMA body phantom filled with 765 MBq lutetium-177 and applied to each patient SPECT dataset.

In addition, venous blood samples of 4 ml were taken at  $5\pm 2$ ,  $15\pm 5$ ,  $30\pm 5$  min,  $1.5\pm 0.5$ ,  $6\pm 1$ ,  $24\pm 3$ ,  $48\pm 3$  h and  $7\pm 1$  d p.i. and their activity concentrations were measured to estimate the radiation dose in the red bone marrow.

## **Dosimetric Analysis**

*Software.* Dosimetric calculations were performed using QDOSE dosimetry software suite (ABX-CRO, Germany) and OLINDA/EXM 1.1 software (18). Dosimetric calculations for the bone tumor lesions were performed using the spherical model in IDAC-Dose 2.1 which accounts for different tissue types including cortical bone (19).

*Image Processing.* All SPECT scans and the corresponding low dose CT images were analyzed with the QDOSE software. The SPECT images were calibrated by applying the calibration factor determined during camera setup. Co-registration between images was verified and manually corrected when necessary.

*Source Organs.* For dosimetric calculations, the following source organs were included: kidneys, red marrow, cortical bone mineral surface, trabecular bone mineral surface, urinary bladder content, and remainder body. Red marrow activity uptake was estimated from venous blood sampling.

*Tumor Definition.* Diagnostic PET/CT images were used to select tumor lesions of interest as well as to determine the lesion volume, using a threshold of 40% of the maximum standardized uptake value (SUVmax) in the PET images (20).

*Retrieval of Activity Values and Time Activity Curves (TACs).* At each time point, activity values were retrieved from the SPECT images using a threshold-based segmentation algorithm for the kidneys (left and right), urinary bladder content, skeleton (excluding tumor regions) and total body. Manual adjustment of the volumes of interest (VOIs) was applied when necessary. The femora were manually excluded from the VOIs for the skeleton. As the segmented VOIs for the total body and the skeleton did not include the legs, the obtained activity values for these organs were scaled by a factor of 1.506 ( $1.506=1/0.664$ ) representing the legs with 33.6% of the total bone mass (21).

Mean activity concentration values and lesion volumes were used to determine the tumor activity values as detailed in the supplemental.

The TACs for source organs and tumor lesions were determined by the activity values and acquisition times of the SPECT scans.

TACs for the red marrow were estimated from venous blood sampling as follows (22):

$$A_{\text{red marrow}} [\text{MBq}] = \frac{AC_{\text{blood}} \left[ \frac{\text{MBq}}{\text{mL}} \right] * \text{RMBLR} * 1500 \text{ g}}{1.05 \frac{\text{g}}{\text{mL}}}$$

Activity (A); activity concentration (AC); red marrow-to-blood activity concentration ratio (RMBLR)

Standard values for the red marrow mass (1500 g) and density (1.05 g/mL) were considered for this estimation. A RMBLR of 1.0 was used as suggested for <sup>177</sup>Lu-therapy (23).

*Activity Integration and Safety Dosimetry.* Organ and tumor lesion TACs were fitted to a sum of exponential functions which were integrated from time 0 to infinity to obtain cumulated activity values. Normalized cumulated activity values were calculated by dividing the cumulated activity by the injected activity. Organ normalized cumulated activity values obtained from QDOSE were used for absorbed and effective dose calculations with OLINDA/EXM 1.1 (18). Additionally, the dose calculator IDAC-Dose 2.1 (19) integrated in QDOSE was used for bone surface dose calculations.

The total kidney mass (considering both kidneys) was individually adapted for dose calculations. Kidney volumes were determined on low-dose CT images and a kidney mass density of 1.06 g/ml was assumed.

As DOTA-ZOL is a bisphosphonate which accumulates in the bone mineral surface (24), the skeleton cumulated activity was distributed between the cortical bone mineral surface (80%) and the trabecular bone mineral surface (20%) (21). Bone surface dose was calculated with IDAC-Dose 2.1 as a representative for the dose to the whole skeleton. A total bone mass for the skeleton of 5500 g was assumed (21). Tumor masses were also individually considered and assumed to have the same mass density as cortical bone (1.92 g/ml) (19).

Maximum tolerated adsorbed doses of 2 Gy (red marrow), 23 Gy (kidneys) and 10 Gy (bone surfaces) were used to determine the dose-limiting organ (25–27).

## **Evaluation of Side Effects and Toxicity**

General safety and adverse effects were assessed at 4 and 10 weeks p.i. by blood biomarkers and according to the Common Terminology Criteria for Adverse Events (CTCAE) version 5.0 (28). A detailed list of biomarkers for inflammation and kidney and liver function is given in the supplemental. Possible hematotoxicity was evaluated by hemoglobin, hematocrit, leukocytes and platelets considering grade 3 and 4 as severe.

## **Statistical Analysis**

All clinical data between baseline and 10 weeks p.i. were compared using the paired Wilcoxon test. Two-sided p values of less than 0.05 ( $p < 0.05$ ) were considered statistically significant. All analyses were performed using Stata software version 14.

## RESULTS

Nine male patients ( $71 \pm 8.6$  y) suffering from mCRPC with exclusive bone metastases were enrolled for evaluation of safety and dosimetry of a therapeutic dose of  $5778 \pm 328.2$  MBq  $^{177}\text{Lu}$ -DOTA-ZOL. One patient was retrospectively excluded from the dosimetry analysis due to strong motion artifacts in the SPECT data.

### Biodistribution

Representative maximum intensity projections of whole-body SPECT images, as well as the mean TACs are presented in Fig. 1. The TACs were expressed as % of injected activity per gram (%IA/g) and not corrected for physical decay of the radionuclide.

#### Fig. 1

Red marrow TACs revealed a fast clearance with low variation within the patient group with mean %IA/g of approximately  $1.4 \cdot 10^{-3}$  %IA/g at 1.5 h p.i. and  $9.7 \cdot 10^{-5}$  %IA/g at 24 h p.i. In contrast, fast uptake and high retention of  $^{177}\text{Lu}$ -DOTA-ZOL was observed in the skeleton. With a peak uptake of  $9.6 \cdot 10^{-3} \pm 2.4 \cdot 10^{-3}$  %IA/g at 2 h p.i. Even at 170 h p.i. the activity in the skeleton was approximately  $3.5 \cdot 10^{-3} \pm 1.3 \cdot 10^{-3}$  %IA/g. The individual skeleton TACs presented a similar shape, with one exception (patient 09) showing a marked increase between 1.5 h and 6 h p.i., The kidney TACs showed large variation within the patients and almost no uptake was observed for the majority of them (6/8).

High retention of  $^{177}\text{Lu}$ -DOTA-ZOL in the tumor lesions with a mean %IA/g of  $2.1 \cdot 10^{-2}$  at 6 h p.i. and approximately  $1.0 \cdot 10^{-2}$  %IA/g at 170 h p.i. was found. However, the shape of the TACs varied not only within the group but also within the same patient, depending on lesion characteristics. Although the highest activity accumulation was found at 6 h p.i. for most lesions, for some of them it was either at 1.5 h p.i. or at 24 h p.i. As a result, the mean standard deviation for each time point was approximately 50%.

Individual TACs are presented in the Supplemental Figs. 1–5.

### Safety Dosimetry

Tab. 1 summarizes the normalized absorbed doses for the organs at risk, namely red marrow, kidneys and skeleton (bone surfaces), and the normalized whole-body effective dose.



## **Tab. 1**

The normalized absorbed doses ranged from 0.206 to 0.564 Gy/GBq for the red marrow, from 0.053 to 0.691 Gy/GBq for the kidneys and from 0.635 to 1.980 Gy/GBq for bone surfaces. The normalized effective doses ranged from 0.095 to 0.216 mSv/MBq. The kidneys showed a much lower normalized absorbed dose compared to the red marrow and the bone surfaces, except for two patients 08 and 09 which presented an elevated kidney uptake.

Assuming a maximum tolerated dose of 2 Gy, 23 Gy and 10 Gy for the red marrow, kidneys and bone surfaces, respectively, the red marrow was the dose-limiting organ for all patients. The maximum safely injectable activity (i.e. activity leading not to surpass any of the defined maximum tolerated doses) ranged from 3.5 GBq to 9.7 GBq with a median of 6.0 GBq.

## **Tumor Dosimetry**

The tumor masses determined from the segmented lesion volumes and an assumed density of 1.92 g/ml are presented in detail in Supplemental Tab. 2. The normalized absorbed doses for the tumor lesions are displayed in Tab. 2.

## **Tab. 2**

The normalized absorbed doses for the tumor lesions ranged from 0.92 to 11.26 Gy/GBq. The mean tumor absorbed doses per patient ranged from 2.61 to 7.99 Gy/GBq. The overall variability (~55%) is acceptable due to the diversity of the lesions (different patients, locations and sizes).

Therapeutic indices were calculated for the red marrow and bone surfaces as the ratio between the mean absorbed doses for the tumor lesions of each patient and the absorbed doses for these organs. Due to the observed low doses, the kidneys were not considered in these calculations. A detailed table with the therapeutic index values is provided (Supplemental Tab. 3). Therapeutic indices ranged from 5.0 to 30.6 when considering the red marrow and from 1.4 to 9.9 when considering the bone surfaces.

Furthermore, dosimetric calculations not considering the skeleton (cortical bone mineral surface and trabecular bone mineral surface) as a source organ were performed for comparison. These results revealed that approximately 70% of the red marrow dose was produced by cross-irradiation from the accumulated activity in the skeleton.

## Evaluation of Safety and Adverse Events

### Fig. 2.

There was no statistically significant effect of the treatment on LDH, ALP, creatinine, hemoglobin or hematocrit levels at any follow-up visit. A significant reduction was observed for leukocytes after 4 and 10 weeks p.i. and for platelets after 4 weeks p.i. ( $p < 0.05$ ). Nevertheless, the initial effect on leukocytes and platelets was transitory and patients showed recovery from week 4 until week 10. We observed grade 3 anemia in 3/9 patients (one already had G3 anemia previously, two had G2) and grade 3 leucopenia in 1/9 patients (from G1 previously). Further, no patient experienced relevant xerostomia, fatigue, nausea, loss of appetite, nephrotoxicity or hepatotoxicity.

### Fig. 3.

## DISCUSSION

Dosimetry and safety evaluation of  $^{177}\text{Lu}$ -DOTA-ZOL were performed in nine patients with mCRPC.

For all patients, the red marrow was the dose-limiting organ, allowing maximum injected activities from 3.5 GBq to 9.7 GBq. Overall, a median injected activity of 6 GBq was calculated as the maximum activity tolerated without exceeding the defined threshold of 2 Gy for the red marrow. However, it should be noted that administration of 6 GBq  $^{177}\text{Lu}$ -DOTA-ZOL may lead to red marrow doses of 3 Gy and higher in some patients. As absorbed doses higher than 3 Gy have been associated with more severe side effects (29), a more conservative treatment administering only 3.5 GBq may guarantee not to exceed a red marrow dose of 2 Gy in any of the patients. Of notice, here a conservative RMBLR value of 1.0 was applied as suggested for  $^{177}\text{Lu}$ -based peptide receptor radionuclide therapy (30). The contribution of red marrow activity to the normalized dose is approximately 30% and therefore a RMBLR value of 0.36, as used in other studies (31), would have resulted in approximately 19% lower absorbed doses. In addition, the presented results are based on calculations using the widely accepted OLINDA/EXM 1.1, which makes specific assumptions for red marrow dose calculations (30). Results calculated with IDAC-Dose 2.1 and IDAC-Dose 1.0 would

have been 12% and 65% higher, respectively (results not shown here). Thus, the use of different dose calculators and/or different assumptions can potentially lead to different results. Furthermore, tumor uptake was excluded from general bone uptake, but, depending on their location, bone lesions may also contribute to red marrow dose, which could have been underestimated in this study. When including the tumor activity as part of the bone activity, the red marrow dose was 8% to 33% (median = 19%) higher. Certainly, to achieve optimal results and to avoid severe side effects, treatment with  $^{177}\text{Lu}$ -DOTA-ZOL should be carefully planned and monitored in a personalized approach in terms of injected activity and number of cycles.

In contrast, the kidneys do not pose a limitation due to their low uptake and fast clearance. With a kidney dose threshold of 23 Gy, the maximum tolerated injected activities ranged from 33.3 GBq to 431.5 GBq.

The tolerable dose limit for the skeleton of 10 Gy may have a high uncertainty as it was determined in a retrospective study without dosimetry (25) and after radiation exposure from a combination of radium-226 ( $\alpha$  emitter) and radium-228 ( $\beta^-$  emitter) (26). Additionally, other authors have suggested different dose thresholds for certain parts of the skeleton (32).

A previous safety dosimetry evaluation for  $^{177}\text{Lu}$ -DOTA-ZOL by Khawar et al. (15) reported absorbed doses to the red marrow, kidneys and osteogenic cells to be 30% higher (mean of 0.461 vs. 0.355 mGy/MBq), 185% higher (0.490 vs. 0.172 mGy/MBq) and 35% lower (3.30 vs. 5.14 mGy/MBq), respectively, compared to this work. Differences of absorbed doses to red marrow and osteogenic cells can be expected due to different assumptions for bone activity calculation. More importantly, the current study has employed 3D SPECT imaging while the dosimetry evaluation by Khawar et al. is based on planar imaging (15). In particular for bone-seeking agents SPECT-based dosimetry has the advantage that the organs and structures of interest can be accurately segmented without including activity from overlapping structures. This also enabled tumor dosimetry which has not been performed previously for  $^{177}\text{Lu}$ -DOTA-ZOL.

In Tab. 3,  $^{177}\text{Lu}$ -DOTA-ZOL is directly compared with other therapeutic radiopharmaceuticals for bone palliation.

**Tab. 3**

Although a direct comparison of multiple radiopharmaceuticals is challenging due to different methodologies,  $^{177}\text{Lu}$ -DOTA-ZOL may have the most favorable therapeutic index compared to the other radiopharmaceuticals (Tab. 3). Furthermore,  $^{177}\text{Lu}$ -DOTA-ZOL shows the second highest tumor-to-bone surface dose ratio after  $^{89}\text{SrCl}_2$ . Accordingly, it can be assumed that  $^{177}\text{Lu}$ -DOTA-ZOL may lead to less bone-related side effects than comparable therapies.

Although the methods applied to define the tumor volumes and activities may lead to additional uncertainties, the obtained tumor doses for  $^{177}\text{Lu}$ -DOTA-ZOL are in the same range as published data for other  $\beta^-$  emitters (except for  $^{89}\text{SrCl}_2$ ) (Tab. 3).

## CONCLUSION

Palliative treatment of bone metastasis using radiolabelled bisphosphonates is proven to be safe and effective.  $^{177}\text{Lu}$ -DOTA-ZOL is a new, theranostic radiotracer for this indication with favorable pharmacokinetics. In this study, we evaluated safety and dosimetry of a single therapeutic dose of  $^{177}\text{Lu}$  DOTA-ZOL showing high uptake and retention in bone lesions. Although  $^{177}\text{Lu}$ -DOTA-ZOL therapy was well tolerated with no observable severe adverse events, the injected activities and the number of administered cycles need to be carefully determined for each patient to avoid severe hematotoxicity. The obtained results and the observed favorable therapeutic index compared to established bone-targeting agents, underline the clinical potential and benefit of  $^{177}\text{Lu}$  DOTA-ZOL for therapy for patients suffering from mCRPC.

## COMPETING INTEREST

The authors declare the following competing financial interest(s): Patent applications on conjugated bisphosphonates for the diagnosis and treatment of bone diseases have been licensed to Isotope Technology Munich (ITM) AG. No other potential conflicts of interest relevant to this article exist.

## ACKNOWLEDGMENTS

The authors would like to thank all of the patients and their families for their participation in the study.

## KEYPOINTS

QUESTION: What was the maximum tolerated injected activity calculated for the dose-limiting organ?

PERTINENT FINDINGS: For all patients treated the red marrow was the dose-limiting organ with a median injected activity of 6 GBq calculated as the maximum activity tolerated. IMPLICATIONS FOR PATIENT CARE: The results of this study and the favorable therapeutic index as compared to established bone-targeting agents, underline the clinical potential of  $^{177}\text{Lu}$ -DOTA-ZOL and its benefit for treatment of patients suffering from mCRPC.

## REFERENCES

1. Hensel J, Thalmann GN. Biology of bone metastases in prostate cancer. *Urology*. 2016;92:6-13.
2. Ulmert D, Solnes L, Thorek DL, Thorek DLJ. Contemporary approaches for imaging skeletal metastasis. *Bone Res*. 2015;3:15024.
3. Frilling A, Weber F, Saner F, et al. Treatment with (<sup>90</sup>)Y- and (<sup>177</sup>)Lu-DOTATOC in patients with metastatic neuroendocrine tumors. *Surgery*. 2006;140:968-76; discussion 976-7.
4. Ahmadzadehfar H, Eppard E, Kürpig S, et al. Therapeutic response and side effects of repeated radioligand therapy with <sup>177</sup>Lu-PSMA-DKFZ-617 of castrate-resistant metastatic prostate cancer. *Oncotarget*. 2016;7:12477-12488.
5. Chakraborty S, Das T, Banerjee S, et al. <sup>177</sup>Lu-EDTMP: a viable bone pain palliative in skeletal metastasis. *Cancer Biother Radiopharm*. 2008;23:202-213.
6. Pfannkuchen N, Meckel M, Bergmann R, et al. Novel radiolabeled bisphosphonates for PET diagnosis and endoradiotherapy of bone metastases. *Pharmaceuticals (Basel)*. 2017;10:45.
7. Agarwal KK, Singla S, Arora G, Bal C. (<sup>177</sup>)Lu-EDTMP for palliation of pain from bone metastases in patients with prostate and breast cancer: a phase II study. *Eur J Nucl Med Mol Imaging*. 2015;42:79-88.
8. Thapa P, Nikam D, Das T, Sonawane G, Agarwal JP, Basu S. Clinical efficacy and safety comparison of <sup>177</sup>Lu-EDTMP with <sup>153</sup>Sm-EDTMP on an equidose basis in patients with painful skeletal metastases. *J. Nucl. Med*. 2015;56:1513-1519.
9. Yuan J, Liu C, Liu X, et al. Efficacy and safety of <sup>177</sup>Lu-EDTMP in bone metastatic pain palliation in breast cancer and hormone refractory prostate cancer: a phase II study. *Clin Nucl Med*. 2013;38:88-92.
10. Meckel M, Bergmann R, Miederer M, Roesch F. Bone targeting compounds for radiotherapy and imaging: \*Me(III)-DOTA conjugates of bisphosphonic acid, pamidronic acid and zoledronic acid. *Radiopharmacy and chemistry*. 2017;1:14.
11. Mirzaei A, Jalilian AR, Badbarin A, et al. Optimized production and quality control of (<sup>68</sup>)Ga-EDTMP for small clinical trials. *Ann Nucl Med*. 2015;29:506-511.
12. Meckel M, Nauth A, Timpe J, et al. Development of a <sup>177</sup>LuBPAMD labeling kit and an automated synthesis module for routine bone targeted endoradiotherapy. *Cancer Biother Radiopharm*. 2015;30:94-99.

13. Dalle Carbonare L, Zanatta M, Gasparetto A, Valenti MT. Safety and tolerability of zoledronic acid and other bisphosphonates in osteoporosis management. *Drug Healthc Patient Saf.* 2010;2:121-137.
14. Khawar A, Eppard E, Roesch F, et al. Preliminary results of biodistribution and dosimetric analysis of [ $^{68}\text{Ga}$ ]Ga-DOTAZOL: a new zoledronate-based bisphosphonate for PET/CT diagnosis of bone diseases. *Ann Nucl Med.* 2019;33:404-413.
15. Khawar A, Eppard E, Roesch F, et al. Biodistribution and post-therapy dosimetric analysis of [ $^{177}\text{Lu}$ ]Lu-DOTAZOL in patients with osteoblastic metastases: first results. *EJNMMI Res.* 2019;9:102.
16. Chopra A. *Molecular Imaging and Contrast Agent Database (MICAD):  $^{68}\text{Ga}$ -labeled (4- $\{(bis(phosphonomethyl))carbamoylemethyl\}$ -7,10-bis(carboxymethyl)-1,4,7,10-tetraazacyclododec-1-yl)acetic acid (BPAMD).* Bethesda (MD); 2004.
17. Pfannkuchen N, Bausbacher N, Pektor S, Miederer M, Rosch F. In vivo evaluation of  $^{225}\text{Ac}$ -DOTAZOL for  $\alpha$ -therapy of bone metastases. *Curr Radiopharm.* 2018;11:223-230.
18. Stabin MG, Sparks RB, Crowe E. OLINDA/EXM: the second-generation personal computer software for internal dose assessment in nuclear medicine. *J. Nucl. Med.* 2005;46:1023-1027.
19. Andersson M, Johansson L, Eckerman K, Mattsson S. IDAC-Dose 2.1, an internal dosimetry program for diagnostic nuclear medicine based on the ICRP adult reference voxel phantoms. *EJNMMI Res.* 2017;7:88.
20. Boellaard R, O'Doherty MJ, Weber WA, et al. FDG PET and PET/CT: EANM procedure guidelines for tumour PET imaging: version 1.0. *Eur J Nucl Med Mol Imaging.* 2010 // 2009;37:181-200.
21. Valentin J. Basic anatomical and physiological data for use in radiological protection: reference values. *Ann ICRP.* 2002;32:1-277.
22. Hindorf C, Glatting G, Chiesa C, Lindén O, Flux G. EANM Dosimetry Committee guidelines for bone marrow and whole-body dosimetry. *Eur J Nucl Med Mol Imaging.* 2010;37:1238-1250.
23. Forrer F, Krenning EP, Kooij PP, et al. Bone marrow dosimetry in peptide receptor radionuclide therapy with  $^{177}\text{Lu}$ -DOTA(0),Tyr(3)octreotate. *Eur J Nucl Med Mol Imaging.* 2009;36:1138-1146.
24. Eppard E, Meisenheimer M, La Fuente A de, Kurpig S, Essler M, Roesch F. Radiolabelling of DOTAMZOL with  $^{68}\text{Ga}$  and  $^{44}\text{Sc}$  for clinical application. *EJEA.* 2016;15:34. doi:10.1530/endoabs.47.OC34.
25. Flux GD. Imaging and dosimetry for radium-223: the potential for personalized treatment. *Br J Radiol.* 2017;90:20160748.

26. Rowland RE. *Radium in humans: A review of U.S. studies*; 1994.
27. Kabasakal L, AbuQbeith M, Aygun A, et al. Pre-therapeutic dosimetry of normal organs and tissues of (<sup>177</sup>)Lu-PSMA-617 prostate-specific membrane antigen (PSMA) inhibitor in patients with castration-resistant prostate cancer. *Eur J Nucl Med Mol Imaging*. 2015;42:1976-1983.
28. U.S. National Cancer Institute. Common Terminology Criteria for Adverse Events 5.0, 1908D. [https://ctep.cancer.gov/protocolDevelopment/electronic\\_applications/docs/CTCAE\\_v5\\_Quick\\_Reference\\_8.5x11.pdf](https://ctep.cancer.gov/protocolDevelopment/electronic_applications/docs/CTCAE_v5_Quick_Reference_8.5x11.pdf). Updated November 27, 2017. Accessed May 8, 2020.
29. Loke KS, Padhy AK, Ng DC, Goh AS, Divgi C. Dosimetric considerations in radioimmunotherapy and systemic radionuclide therapies: A review. *World J Nucl Med*. 2011;10:122.
30. Stabin MG, Siegel JA, Sparks RB, Eckerman KF, Breitz HB. Contribution to red marrow absorbed dose from total body activity: a correction to the MIRD method. *J. Nucl. Med*. 2001;42:492-498.
31. Delker A, Fendler WP, Kratochwil C, et al. Dosimetry for (<sup>177</sup>)Lu-DKFZ-PSMA-617: a new radiopharmaceutical for the treatment of metastatic prostate cancer. *Eur J Nucl Med Mol Imaging*. 2016;43:42-51.
32. Emami B, Lyman J, Brown A, et al. Tolerance of normal tissue to therapeutic irradiation. *Int J Radiat Oncol Biol Phys*. 1991;21:109-122.
33. Robinson RG, Blake GM, Preston DF, et al. Strontium-89: treatment results and kinetics in patients with painful metastatic prostate and breast cancer in bone. *Radiographics*. 1989;9:271-281.
34. Sharma S, Singh B, Koul A, Mittal BR. Comparative therapeutic efficacy of <sup>153</sup>Sm-EDTMP and <sup>177</sup>Lu-EDTMP for bone pain palliation in patients with skeletal metastases: patients' pain score analysis and personalized dosimetry. *Front Med (Lausanne)*. 2017;4:46.
35. Liepe K, Hliscs R, Kropp J, Runge R, Knapp FF, Franke W-G. Dosimetry of <sup>188</sup>Re-hydroxyethylidene diphosphonate in human prostate cancer skeletal metastases. *J. Nucl. Med*. 2003;44:953-960.
36. Pacilio M, Ventroni G, Vincentis G de, et al. Dosimetry of bone metastases in targeted radionuclide therapy with alpha-emitting (<sup>223</sup>)Ra-dichloride. *Eur J Nucl Med Mol Imaging*. 2016;43:21-33.
37. Lassmann M, Eberlein U. Targeted alpha-particle therapy: imaging, dosimetry, and radiation protection. *Ann ICRP*. 2018;47:187-195.



346 38. Atkins HL, Srivastava SC. Radiopharmaceuticals for bone malignancy therapy. *J Nucl Med Technol.*  
347 1998;26:80-3; quiz 85-6.  
348

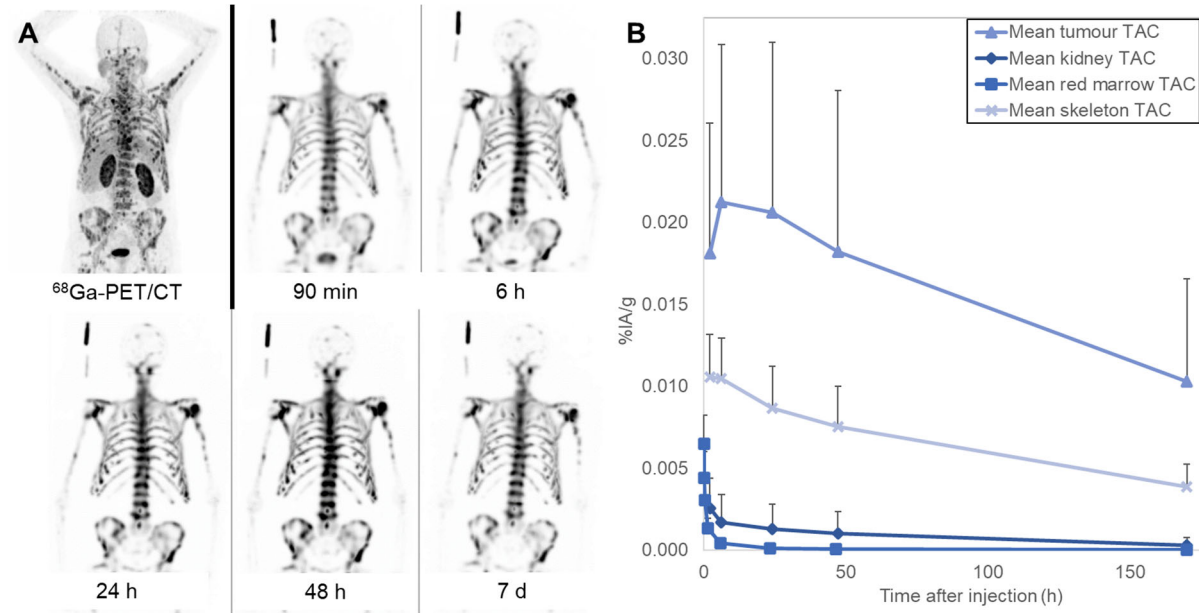
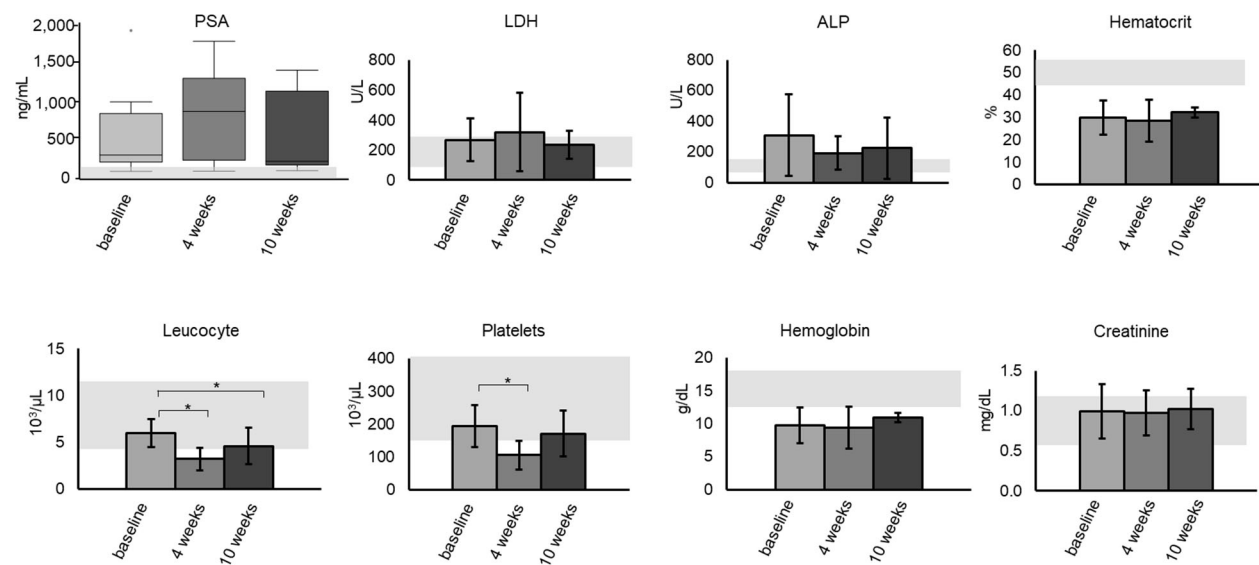


Fig. 1: A: maximum-intensity projections of a PET/CT scan and of whole-body SPECT images at 1.5, 6, 24, 48 h and 7 d p.i. for a representative patient (patient 06). B: TACs for red marrow, kidneys, skeleton and tumor lesions expressed as %IA/g.

354



355  
356 Fig. 2: Selected biomarkers at baseline, four and ten weeks p.i. Grey areas represent norm values, \* $p < 0.05$ , the point  
357 at baseline PSA represents an outlier (patient 04).

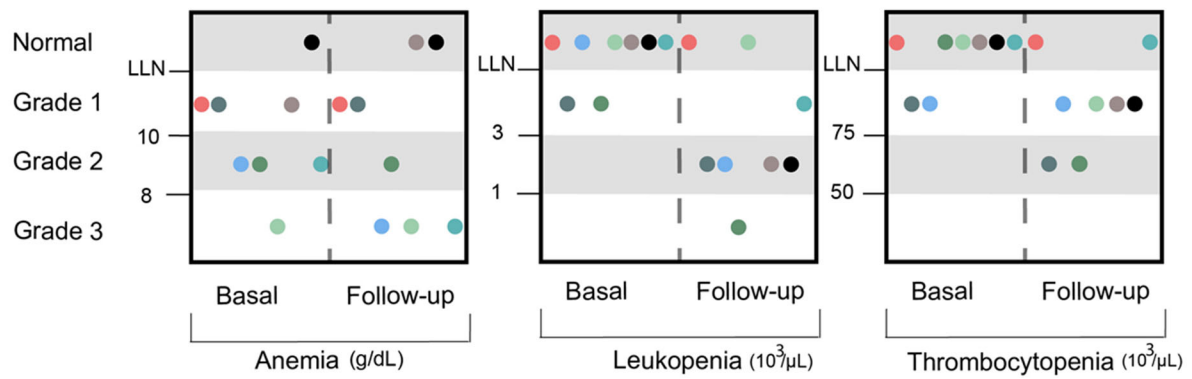


Fig. 3: Survey of adverse events according to CTCAE v5.0 (28) for 8/9 patients before (basal) and at 10 weeks after treatment (follow-up).

361 TABLES

362 Tab. 1: Normalized absorbed doses for the organs at risk [Gy/GBq] and normalized effective dose [mSv/MBq].

	Patient ID										
Organ	01	02	03	04	06	07	08	09	Median	Mean	SD
Red marrow	0.326	0.346	0.564	0.499	0.301	0.206	0.226	0.375	0.336	0.355	0.116
Kidneys	0.063	0.097	0.054	0.053	0.078	0.094	0.250	0.691	0.086	0.172	0.205
Bone surfaces	1.080	1.180	1.980	1.780	1.040	0.635	0.641	1.220	1.130	1.195	0.450
Effective dose	0.143	0.130	0.216	0. <sup>177</sup>	0.109	0.095	0.106	0.158	0.137	0.142	0.038
Dose-limiting organ	Red marrow										
Maximum tolerated injected activity (GBq)	6.1	5.8	3.5	4.0	6.6	9.7	8.8	5.3	6.0	6.3	2.0

363

364 Tab. 2: Normalized tumor doses [Gy/GBq]. For patient 09 only four lesions were defined.

Patient ID									Overall tumor statistics		
Lesion	01	02	03	04	06	07	08	09	Median	Mean	SD
1	5.02	5.15	3.63	2.85	2.03	8.05	6.13	7.94	3.63	4.21	2.40
2	2.37	3.70	3.00	3.86	2.52	8.94	3.44	11.26*			
3	5.37	1.72	1.65	2.25	2.79	3.69	1.17	9.27			
4	6.98	0.92	1.66	5.91	3.54	6.57	3.26	3.51			
5	2.53	1.56	4.10	4.39	4.36	4.26	2.84	NA			
Median	5.02	1.72	3.00	3.86	2.79	6.57	3.26	8.60			
Mean	4.45	2.61	2.81	3.85	3.05	6.30	3.37	7.99			
SD	1.77	1.57	1.00	1.27	0.82	2.05	1.60	2.85			

365 \*Calculated with SPECT activity threshold of 82% SUVmax as the volume determined with a threshold of 50%

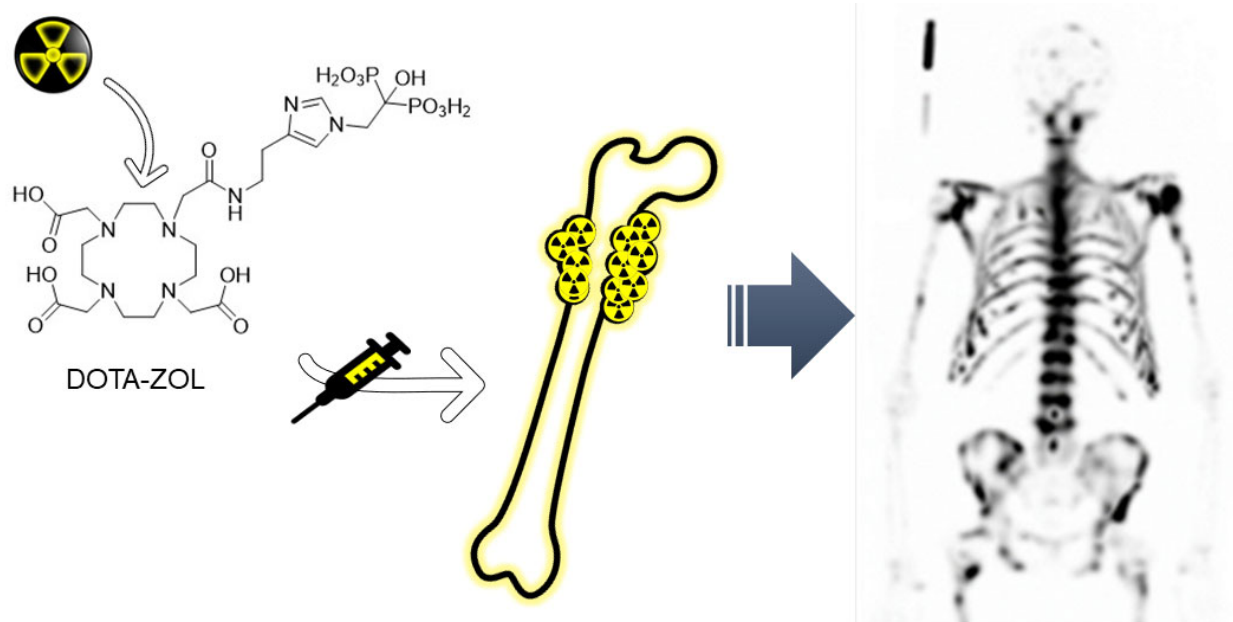
366 SUVmax showed a very large difference with the volume determined in the pre-therapeutic PET image.

Tab. 3: Comparison of  $^{177}\text{Lu}$ -DOTA-ZOL to other radiopharmaceuticals used for bone metastasis treatment. Values are normalized absorbed doses [Gy/GBq] as mean $\pm$ SD. Tumor-to-red-marrow dose ratio and tumor-to-bone surface dose ratio were calculated as the mean of the dose ratios for each patient.

	$^{177}\text{Lu}$ - DOTA-ZOL	$^{89}\text{SrCl}_2^{\text{a}(33)}$	$^{153}\text{Sm}$ - EDTMP $^{\text{b}(34)}$	$^{177}\text{Lu}$ - EDTMP $^{\text{b}(34)}$	$^{188}\text{Re}$ - HEDP $^{\text{c}(35)}$	$^{223}\text{Ra-Cl}_2^{\text{d}}$
<b>Tumor lesion</b>	4.21 $\pm$ 2.40	233 $\pm$ 166	6.22 $\pm$ 4.21	6.92 $\pm$ 3.92	3.83 $\pm$ 2.01	179.8 (68-490) $^{(36)}$
<b>Red marrow</b>	0.36 $\pm$ 0.12	18.9	1.41 $\pm$ 0.6	0.83 $\pm$ 0.21	0.61 $\pm$ 0.21	73.9 $^{(37)}$
<b>Bone surface</b>	1.19	30.2	7.8	NA	1.403	739.1 $^{(37)}$
<b>Tumor-to-red- marrow dose ratio</b>	13.9	12.3	4.40	8.31	6.28	2.4
<b>Tumor-to-bone- surface dose ratio</b>	3.5	7.7	0.8	NA	2.7	0.2
<b>Dose-limiting organ</b>	Red marrow					

Bone surface dose estimated using a bone-to-red marrow dose ratios of  $^{\text{a}}$ 1.6 (38),  $^{\text{b}}$ 5.5 (38) and  $^{\text{c}}$ 2.3 (for  $^{186}\text{Re}$ -HEDP) (38).  $^{\text{d}}$ Radium-223 is an  $\alpha$ -emitter, therefore a RBE factor of 5 needs to be applied for comparison with  $\beta$ -emitters (RBE=1).

373 GRAPHICAL ABSTRACT



374



# Supplemental Material

*Rene Fernandez<sup>a</sup>, Elisabeth Eppard<sup>b</sup>, Wencke Lehnert<sup>c,d</sup>, Luis David Jiménez-Franco<sup>c</sup>, Cristian Soza-Ried<sup>a</sup>, Matias Ceballos<sup>a</sup>, Jessica Ribbeck<sup>b</sup>, Andreas Kluge<sup>c</sup>, Frank Rösch<sup>c</sup>, Marian Meckelf, Konstantin Zhernosekov<sup>f</sup>, Vasko Kramer<sup>a,b</sup> and Horacio Amaral<sup>a,b</sup>*

<sup>a</sup>Center for Nuclear Medicine & PET/CT Positronmed, Santiago, Chile

<sup>b</sup>Positronpharma SA, Santiago, Chile

<sup>c</sup>ABX-CRO, Dresden, Germany

<sup>d</sup>Department of Nuclear Medicine, University Medical Center Hamburg, Germany

<sup>e</sup>Institute of Nuclear Chemistry, Johannes Gutenberg-University, Mainz, Germany

<sup>f</sup>Isotope Technologies Garching GmbH, Munich, Germany

KEYWORDS: Bone metastasis; Bisphosphonate, <sup>177</sup>Lu-DOTA-ZOL, Radionuclide therapy, Dosimetry

## METHODS

### Preparation of $^{177}\text{Lu}$ -DOTA-ZOL

Radiolabelling of  $^{177}\text{Lu}$ -DOTA-ZOL was performed by adding 160  $\mu\text{g}$  (228 nmol) DOTA-ZOL dissolved in 1.0 mL ascorbate buffer pH 4.5 to non-carrier-added lutetium-177 obtained from ITG (Isotope Technologies Garching GmbH, Garching, Germany) and heating to 95°C for 30 min. The reaction was diluted with 0.9% sodium chloride and passed through a 0.22  $\mu\text{m}$  sterile filter. Quality control was carried out with an aliquot of the final product with silica-gel coated aluminum TLC-plates (silica 60 F254.5x4.5 cm, Merck, Darmstadt, Germany). Analysis was performed with a single trace radioTLC-scanner (PET-miniGITA, Elysia-Raytest, Straubenhardt, Germany) and evaluation software (Gina Star TLC, Elysia-Raytest, Straubenhardt, Germany). Development of two TLC-plates was conducted in two different solvent systems: 0.1 M citrate buffer (pH 4) and a mixture of acetylacetone, acetone and concentrated HCl (1:1:0.1). In citrate buffer,  $^{177}\text{Lu}$ -DOTA-ZOL was found at a retention factor ( $R_f$ ) of  $R_f = 0-0.1$  and free unlabeled lutetium-177 at  $R_f = 1.0$ . In the organic solvent system,  $^{177}\text{Lu}$ -DOTA-ZOL was found at  $R_f = 0.0-0.1$  and free unlabeled lutetium-177 at  $R_f = 0.8-1.0$ . A radiochemical yield  $\geq 95\%$  and a radiochemical purity  $\geq 98\%$  was obtained.

### Patient data

The presence of bone metastasis and absence of visceral metastasis was verified by  $^{68}\text{Ga}$ -PSMA-11 (n=2) or  $^{18}\text{F}$ -PSMA-1007 (n=7) PET/CT scans within one week prior to therapy. Also, the patients had positive bone scans ( $^{68}\text{Ga}$ -NODAGA-ZOL PET or  $^{99\text{m}}\text{Tc}$ -MDP SPECT) prior to recruitment into the study.

Tab. 1: Patient characteristics, blood biomarkers and injected  $^{177}\text{Lu}$ -DOTA-ZOL for the treatment.

	Mean $\pm$ SD	Range	Reference range
<b>Patients</b>			
Age	70.8 $\pm$ 8.36	57-82	NA
ECOG baseline	1.00 $\pm$ 1.00	0-2	0
EVA baseline	2.33 $\pm$ 1.73	0-5	0
PSA baseline (ng/mL)	538.77 $\pm$ 625.1	13.5-1964	<4.0
<b>Blood biomarkers at baseline</b>			
Erythrocytes ( $10^6/\mu\text{L}$ )	3.35 $\pm$ 0.83	1.64-4.59	4.7-6.1
Hemoglobin (g/dL)	9.77 $\pm$ 2.69	4.1-14.0	14.0-18.0
Hematocrit (%)	29.8 $\pm$ 7.69	13.3-40.6	42.0-52.0
Leukocytes ( $10^3/\mu\text{L}$ )	5.99 $\pm$ 1.49	3.46-8.10	4.5-11.0
Platelets ( $10^3/\mu\text{L}$ )	193 $\pm$ 64	102-316	140-400
ESR (mm/hr)	40.6 $\pm$ 39.6	12-140	1-15
ALP (U/L)	309 $\pm$ 266	102-694	40-130
GGT (U/L)	110 $\pm$ 136	10-367	15-73
LDH (U/L)	268 $\pm$ 143	126-595	0-250
Creatinine (mg/dL)	1.00 $\pm$ 0.34	0.64-1.71	0.7-1.2
<b>Injected dose</b>			
$^{177}\text{Lu}$ -DOTA-ZOL (MBq)	5780 $\pm$ 329	5215-6380	

## Retrieval of activity values for tumor lesions

Mean activity concentration values and lesion volumes were used to determine the tumor activity values. The latest SPECT imaging time point (7 d p.i.) was selected for the definition of a reference volume for activity concentration calculation as the signal-to-background ratio was expected to be maximal for this time-point. A threshold of 50% SUVmax in the region of the lesion was used to determine the reference volume for the activity concentration calculations, which was found suitable to separate the tumor signal from the background considering the spatial resolution of  $^{177}\text{Lu}$ -SPECT imaging. The shape of the tumor VOIs were adapted through the time-points in order to maximize the retrieved activity (conserving the same volume) as the tumor signal was expected to be considerably higher than the background in all time-points. Subsequently, activity concentration values for each lesion were calculated using the retrieved activity and the reference volume. Total tumor activities for each time-point were calculated by multiplying the activity concentration values by the lesion volume as defined by the PET images. In the

cases when the PET-based volumes were smaller than the reference volumes, the total activity values for the lesions were defined by the 50% SUV<sub>max</sub> in the SPECT images.

### **Evaluation of Side Effects and Toxicity**

Alanine aminotransferase (ALT), alkaline phosphatase (ALP), aspartate aminotransferase (AST), creatinine (CRE), erythrocyte sedimentation rate (ESR), gamma-glutamyl transferase (GGT), lactate dehydrogenase (LDH) and total bilirubin (TBIL) were used as biomarkers of inflammation, kidney and liver function. Possible hematotoxicity was evaluated by hemoglobin, hematocrit, leukocytes and platelets as biomarkers considering grade 3 and 4 as severe.

## **RESULTS**

### **Biodistribution**

The following figures (Fig. 1 to 5) present the individual TACs determined for each patient expressed as % of injected activity per gram (%IA/g) over time in a logarithmic plot. The TACs were not corrected for physical decay. The individual tumor TACs were calculated as the mean of five selected osteoblastic tumor lesions and presented together with the corresponding standard deviation. For patient 09 only four tumor lesions were defined. Patient 05 needed to be retrospectively excluded from the dosimetric evaluation and therefore TACs for this patient are not presented.

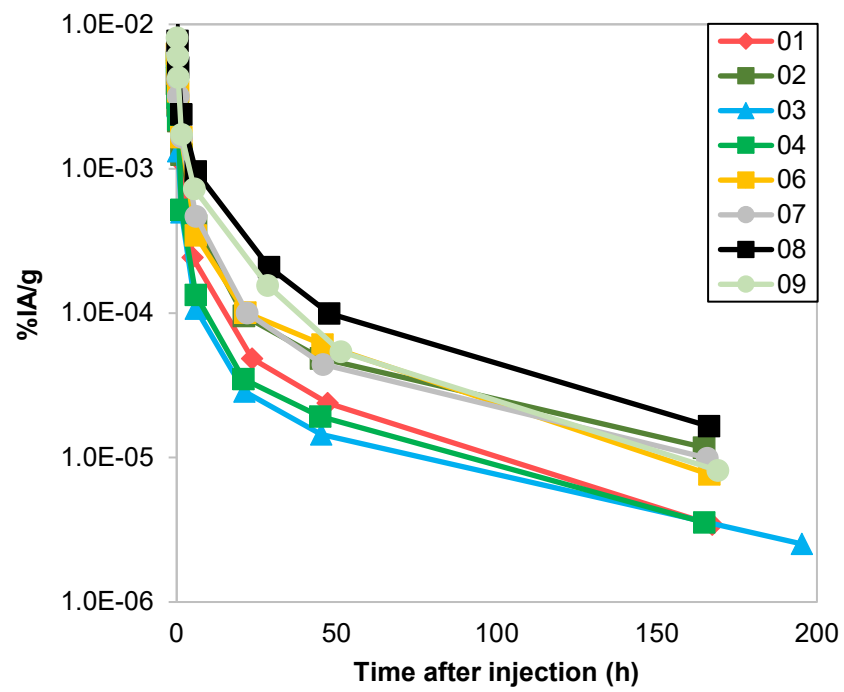


Fig. 1: Individual TACs for red marrow expressed as percentage of injected activity per gram (%IA/g). A red marrow mass of 1500 g was assumed (1).

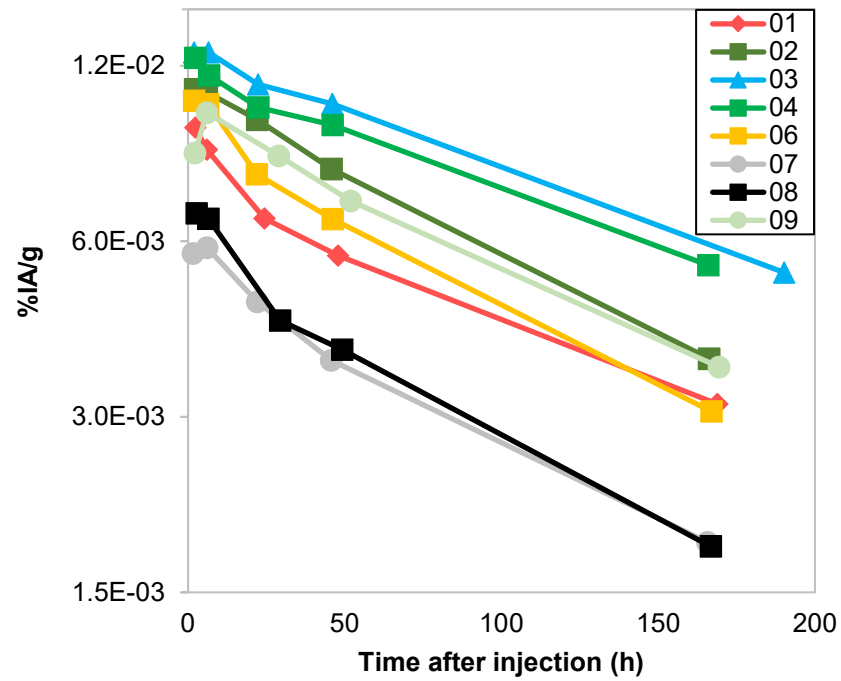


Fig. 2: Individual TACs for the skeleton without tumor regions expressed as percentage of injected activity per gram (%IA/g). A skeleton mass of 5500 g was assumed (2).

Patient 09 exhibited a significant increase of approximately 10% between 1.5 h p.i and 6 h p.i. for the skeleton TACs.

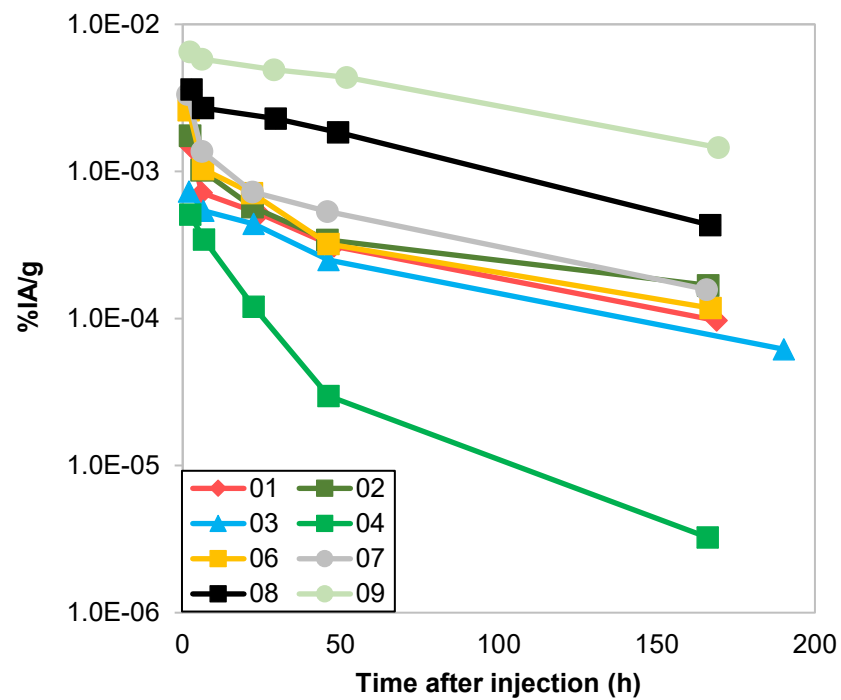


Fig. 3: Individual TACs for the kidney expressed as percentage of injected activity per gram (%IA/g). A density of 1.06 g/ml was assumed for the calculation of the individual kidney masses.

For the kidney TACs, patients 08 and 09 showed a relatively high uptake (patient 08: 3.5-fold higher; patient 09: 12-fold higher) compared to the other patients that presented almost no uptake.

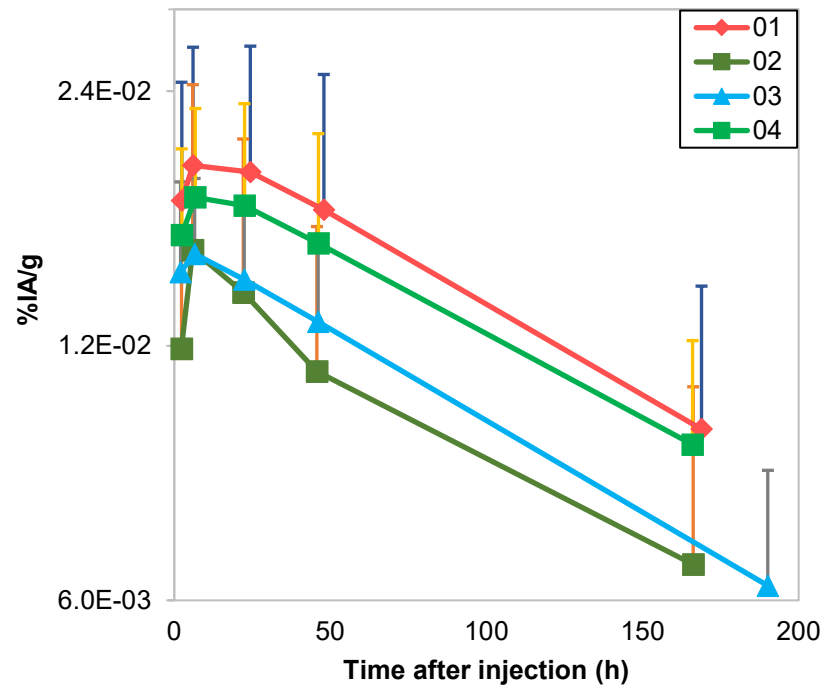


Fig. 4: Individual mean tumor TACs expressed as percentage of injected activity per gram of tumor (%IA/g) of patients 01-04. Standard deviation of the accumulation in the lesions is represented as a vertical bar, but only with the positive direction to improve and clarify the graphical appearance.



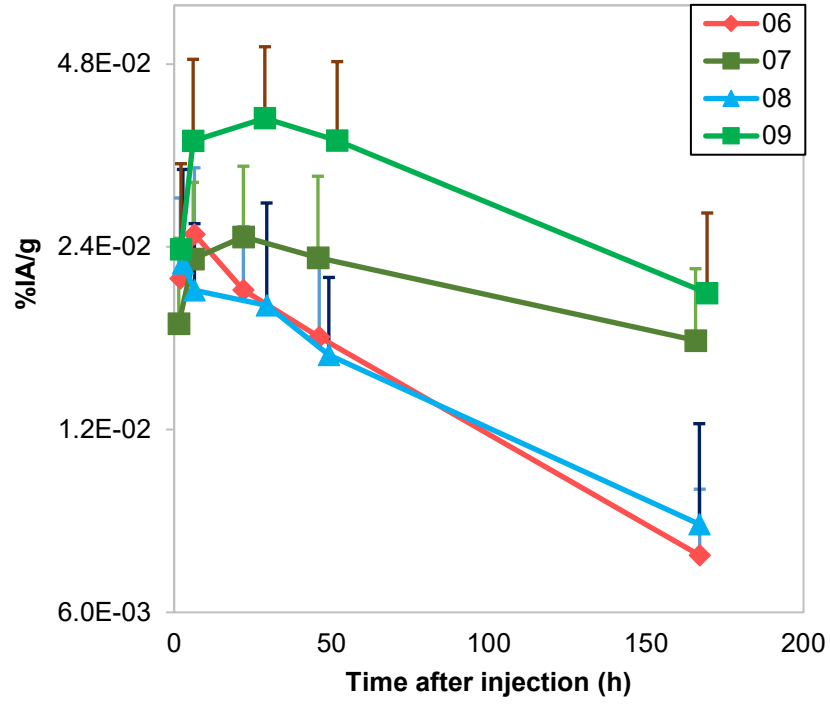


Fig. 5: Individual mean tumor TACs expressed as percentage of injected activity per gram of tumor (%IA/g) of patients 06-09. Standard deviation of the accumulation in the lesions is represented as a vertical bar, but only with the positive direction to improve and clarify the graphical appearance.

## Tumor Dosimetry

The tumor masses determined from the obtained lesion volumes and an assumed density of 1.92 g/ml are presented in Tab. 2. For patient 09 only four lesions were defined.

Tab. 2: Masses of the selected osteoblastic tumor lesions determined with an assumed density of 1.92 g/ml (cortical bone).

Patient ID	Tumor mass [g]							
	01	02	03	04	06	07	08	09
<b>Lesion 1</b>	11.98	0.96	21.41	5.26	14.02	5.74	0.63	18.45
<b>Lesion 2</b>	4.97	4.78	17.70	28.03	7.01	0.79	8.79	4.42
<b>Lesion 3</b>	2.17	9.56	15.28	4.15	2.07	1.27	2.94	33.14
<b>Lesion 4</b>	40.90	3.97	11.71	20.54	1.92	2.71	1.65	2.50
<b>Lesion 5</b>	28.28	14.17	99.24	13.69	5.41	3.67	10.83	N/A

Calculated therapeutic indices are presented in Tab. 3 for red marrow and bone surface as the ratio between the mean absorbed doses determined for the tumor lesions of each patient and the absorbed doses for these organs. Due to the observed low doses, the kidneys were not considered in these calculations.

Tab. 3: Therapeutic indices between mean tumor absorbed dose and absorbed doses for red marrow and bone surface calculated for each patient.

Organ	Patient ID								Median	Mean	SD
	01	02	03	04	06	07	08	09			
<b>Red marrow</b>	13.7	7.5	5.0	7.7	10.1	30.6	14.9	21.3	11.9	13.9	8.0
<b>Bone surface</b>	4.1	2.2	1.4	2.2	2.9	9.9	5.3	6.6	3.5	4.3	2.7

## REFERENCES

1. Forrer F, Krenning EP, Kooij PP, et al. Bone marrow dosimetry in peptide receptor radionuclide therapy with  $^{177}\text{Lu}$ -DOTA(0),Tyr(3)octreotate. *Eur J Nucl Med Mol Imaging*. 2009;36:1138-1146.
2. Valentin J. Basic anatomical and physiological data for use in radiological protection: reference values. *Ann ICRP*. 2002;32:1-277.